Supplementary Information

Molecular characterization of ulcerative colitis-associated colorectal carcinomas

Daniela Hirsch[1,2], Julia Hardt[3], Christian Sauer[1], Kerstin Heselmeyer-Hadded[2], Stephanie H. Witt [4], Peter Kienle[5], Thomas Ried[2], Timo Gaiser[1]

[1] Institute of Pathology, University Medical Center Mannheim, Medical Faculty Mannheim, Heidelberg University, Mannheim, Germany

[2] Cancer Genomics Section, Genetics Branch, Center for Cancer Research, National Cancer Institute, National Institutes of Health, Bethesda, MD, USA

[3] Department of Surgery, University Medical Center Mannheim, Medical Faculty Mannheim, Heidelberg University, Mannheim, Germany

[4] Department of Genetic Epidemiology in Psychiatry, Central Institute of Mental Health, Medical Faculty Mannheim, Heidelberg University, Mannheim, Germany

[5] General and Visceral Surgery, Theresienkrankenhaus and St. Hedwig-Klinik GmbH, Mannheim, Germany

Supplementary Table

Supplementary Table S1. Clinico-pathologic characteristics of individual UC-CRC cases.

Supplementary Figures

Supplementary Figure S1. Variety of histomorphologies of ulcerative colitis-associated colorectal carcinomas.

Supplementary Figure S2. Distribution and cumulative frequency of copy number alterations in CRCs with intestinal-type or mucinous histology from the TCGA cohort.

Supplementary Figure S3. Graphical summary of *TP53* mutations from ulcerative colitis associated colorectal carcinomas (n = 23) mapped on the linear protein and its domains from Pfam (Protein family database from Wellcome Trust Sanger Institute; lollipop plot).

Supplementary Figure S4. Available molecular data per patient.

Supplementary Figure S5. Overview of all detected mutations in ulcerative colitis patients with synchronous carcinomas.

Supplementary Figure S6. Morphologic (H&E, *left*) and immunohistochemical (TP53, *right*) alterations in colonic mucosa surrounding the carcinoma spot (indicated by black dot in the schematic, sampled surrounding mucosa area is highlighted light orange) of patient UC02.

Supplementary Figure S7. Morphologic (H&E, *left*) and immunohistochemical (TP53, *right*) alterations in mucosa surrounding the carcinoma spot (indicated by black dot in the schematic, sampled surrounding mucosa area is highlighted light orange) of patient UC03.

Supplementary Figure S8. Morphologic (H&E, *left*) and immunohistochemical (TP53, *right*) alterations in colonic mucosa in spatial proximity but not adjacent to the carcinoma spot (indicated by black dot in the schematic, sampled mucosa area is highlighted light orange) of patient UC06.

Supplementary Figure S9. Morphologic (H&E, *left*) and immunohistochemical (TP53, *right*) alterations in colonic mucosa surrounding the carcinoma spot (indicated by black dot in the schematic, sampled surrounding mucosa area is highlighted light orange) of patient UC07.

Supplementary Figure S10. Morphologic (H&E, *left*) and immunohistochemical (TP53, *right*) alterations in colonic mucosa surrounding the carcinoma spot (indicated by black dot in the schematic, sampled surrounding mucosa area is highlighted light orange) of patient UC09.

Supplementary Figure S11. Morphologic (H&E, *left*) and immunohistochemical (TP53, *right*) alterations in the carcinoma (indicated by black dot in the schematic) and adjacent colonic mucosa (highlighted in light orange in the schematic) of patient UC18.

Supplementary Table

Supplementary Table S1. Clinico-pathologic characteristics of individual UC-CRC cases.

Patient number	Specimen ID	Age at CRC diagnosis, years	Duration of UC at CRC diagnosis, years	Sex	AJCC stage at diagnosis[1]	Site of (primary) carcinoma	Special histology	Microsatellite status
1	UC01CA	76	N/A	male	II	sigmoid colon	no	MSS
2	UC02CAis	59	14	female	0	cecum	no	MSS
3	UC03CA	51	34	female	I	ascending colon	mucinous, signet ring	MSS
4	UC04CA	29	13	female	IV	rectum	mucinous, signet ring	MSS
5	UC05CA1	41	21	male	III	ascending colon	no	MSS
5	UC05CA2	41	21	male	III	cecum	no	MSS
5	UC05CA3	41	21	male	III	hepatic flexure	no	MSS
6	UC06CA	47	20	female	II	sigmoid colon	no	MSS
7	UC07CA	34	16	female	I	sigmoid colon	mucinous	MSS
8	UC08CA1	44	N/A	female	II	transverse colon	no	MSS
8	UC08CA2	44	N/A	female	II	transverse colon	mucinous	MSS
9	UC09CAis	31	8	male	0	rectum	no	MSS
10	UC10CA1	45	26	female	III	rectum	no	MSS
10	UC10CA2	45	26	female	III	sigmoid colon	no	MSS
11	UC11CA	64	N/A	male	I	rectum	no	MSS
12	UC12CA1	58	33	male	I	rectosigmoid junction	no	MSS
12	UC12CA2	58	33	male	I	rectum	no	MSS
13	UC13CA	43	20	male	III	cecum	no	MSS
14	UC14CA	38	15	female	II	descending colon	no	MSS
15	UC15CA	49	3	male	I	rectum	no	MSS
16	UC16CA	51	15	male	III	ascending colon	mucinous	MSS
17	UC17CA	34	7	female	I	sigmoid colon	no	MSS
18	UC18CA	33	21	male	III	cecum	mucinous	MSS
19	UC19CA	64	30	male	III	rectum	mucinous	MSS

[1]AJCC stages are based on pathology assessment of the oncologic resection specimen.
CA, carcinoma; CRC, colorectal cancer; DYS, dysplasia; is, in situ; MSS, microsatellite stable; N/A, data not available; UC, ulcerative colitis.

Supplementary Figures

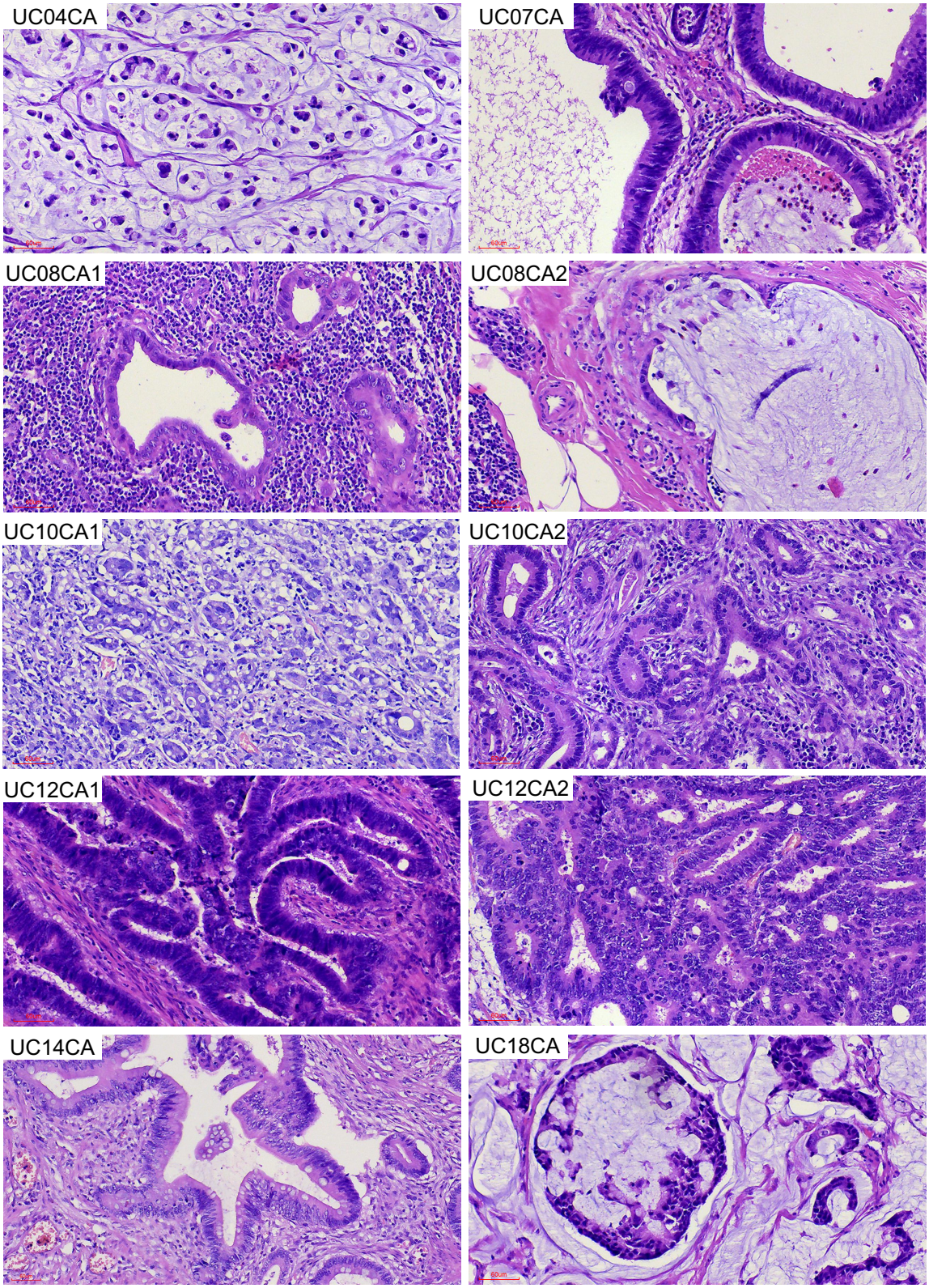

Supplementary Figure S1. Variety of histomorphologies of ulcerative colitis-associated colorectal carcinomas. Histotypes comprise signet ring cell carcinoma (UC04CA), adenocarcinomas with mucinous differentiation (UC07CA, UC08CA2, UC18CA), and intestinal-type adenocarcinomas with different degrees of differentiation and inflammatory infiltrate (UC08CA1, UC10CA1, UC10CA2, UC12CA1, UC12CA2, UC14CA). H&E staining, 20x objective, scale bar 60 µm.

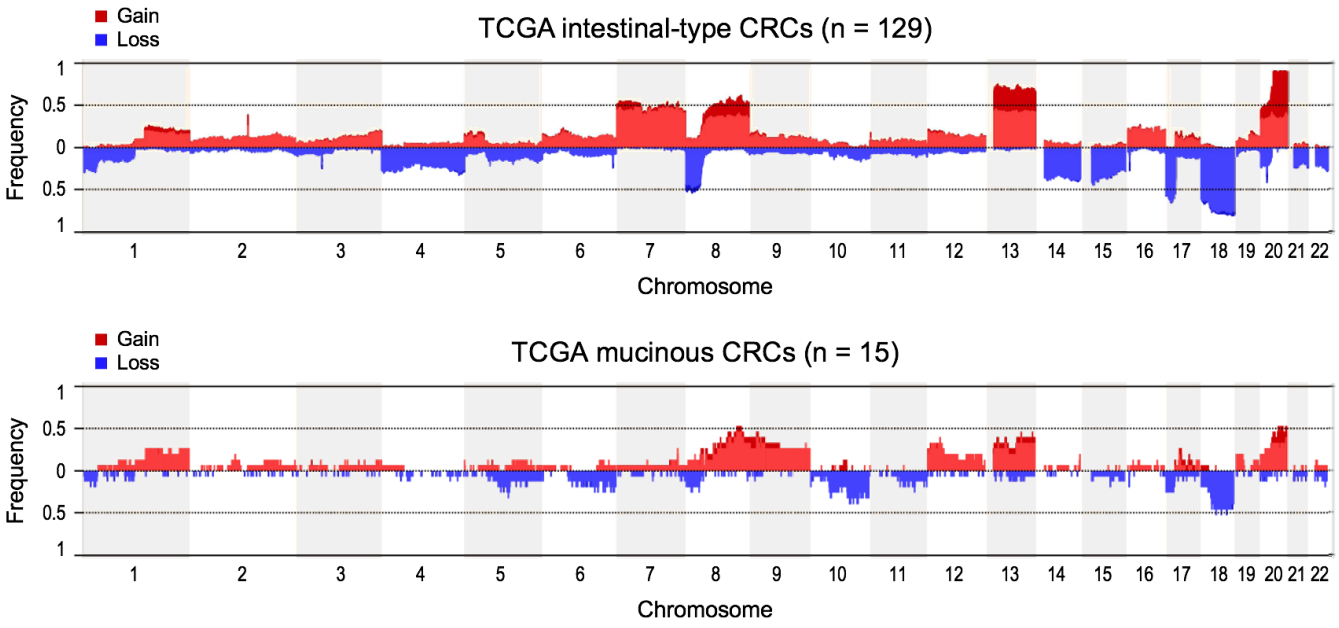

Supplementary Figure S2. Distribution and cumulative frequency of copy number alterations in CRCs with intestinal-type or mucinous histology from the TCGA CRC cohort (2012). The frequency of copy number alterations tends to be higher in intestinal-type than in mucinous CRCs. Numbers below the graph (x-axis) denote chromosomes, frequency (y-axis) denotes the proportion of samples with a gain or a loss at the respective chromosomal position. Only microsatellite stable/non-hypermutated samples were included in this analysis. In contrast to UC-CRCs, gains of chromosome arm 5p are infrequent.

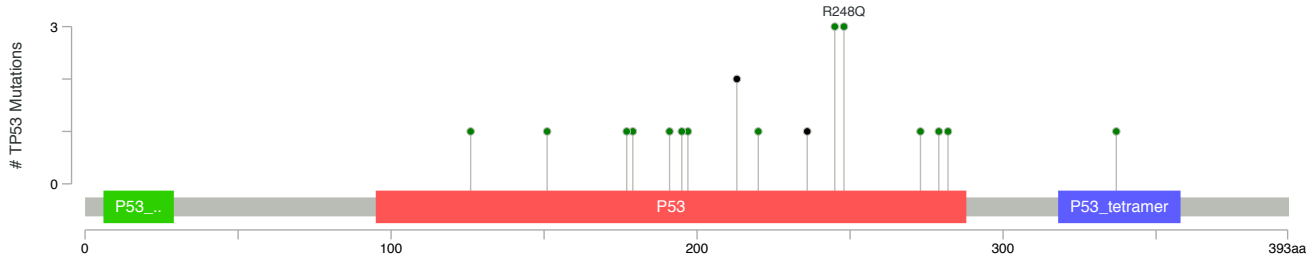

Supplementary Figure S3. Graphical summary of *TP53* mutations from ulcerative colitis associated colorectal carcinomas (n = 23) mapped on the linear protein and its domains from Pfam (Protein family database from Wellcome Trust Sanger Institute; lollipop plot). The different domains of TP53 are marked in color: TP53 transactivation motif (5 – 29) in green, TP53 DNA binding domain (95 – 289) in red and TP53 tetramerisation motif (319 – 358) in blue. 'Lollipops': green, missense mutation; black, truncating mutation.

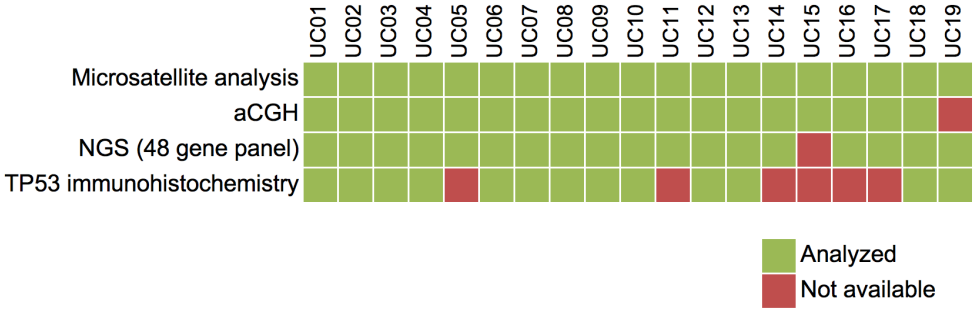

Supplementary Figure S4. Available molecular data per patient. In two cases, sequencing or aCGH failed due to insufficient DNA quality and/or amount. Similarly, no sufficient tissue was left for immunohistochemical analysis of TP53 for some cases. aCGH, array-based comparative genomic hybridization; NGS, next generation sequencing.

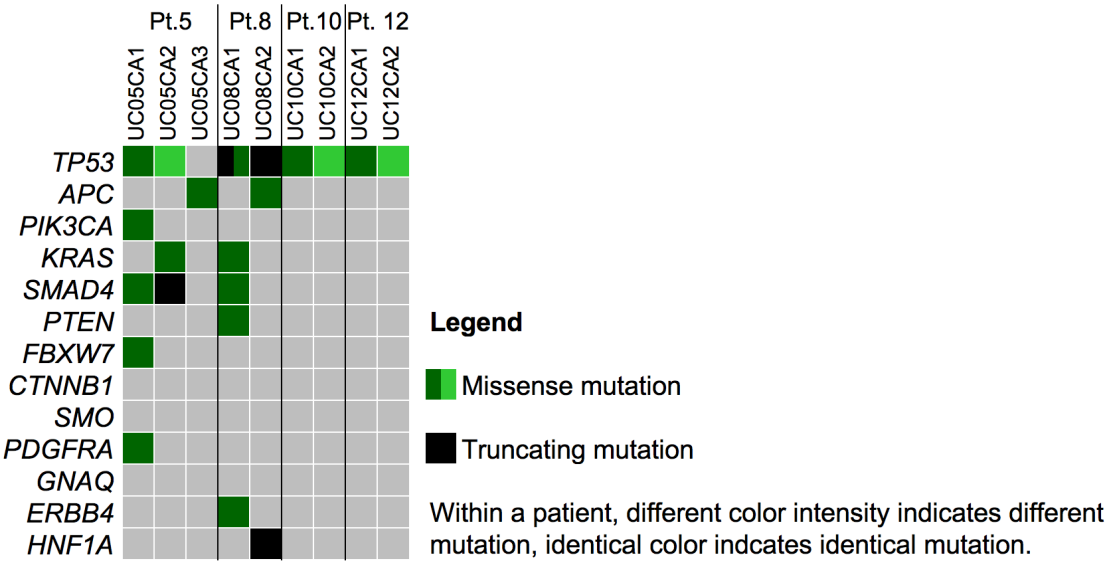

Supplementary Figure S5. Overview of all detected mutations in ulcerative colitis patients with synchronous carcinomas. Although eight of nine synchronous UC-CRCs from individual patients had a mutation in *TP53*, the specific TP53 mutations of the respective tumors were usually distinct.

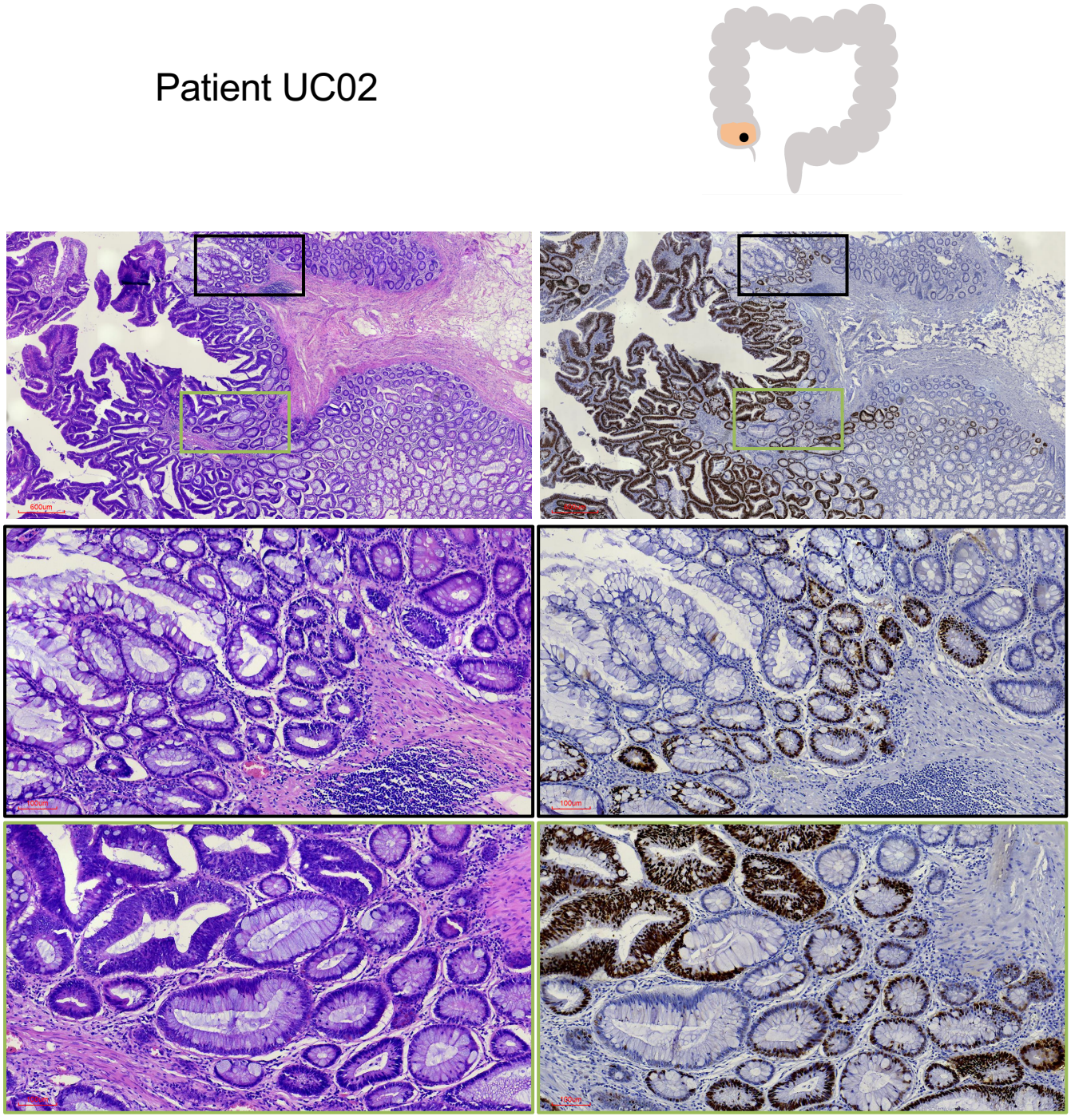

Supplementary Figure S6. Morphologic (H&E, *left*) and immunohistochemical (TP53, *right*) alterations in colonic mucosa surrounding the carcinoma spot (indicated by black dot in the schematic, sampled surrounding mucosa area is highlighted light orange) of patient UC02. Histology shows inflamed, non-dysplastic mucosa along with low-grade and high-grade dysplasia. Dysplastic glands show an aberrant TP53 immunostaining presenting as a 'diffuse pattern' with strongly positive cells in most areas of the glands, indicative of a *TP53* mutation. Some non-dysplastic glands in spatial proximity to the dysplastic lesion also display an aberrant TP53 immunostaining in the basal half of the crypts (so-called 'nested pattern'). The adjacent carcinoma harbors a *TP53* mutation (p.P191L), suggesting tumor progression through field cancerization.

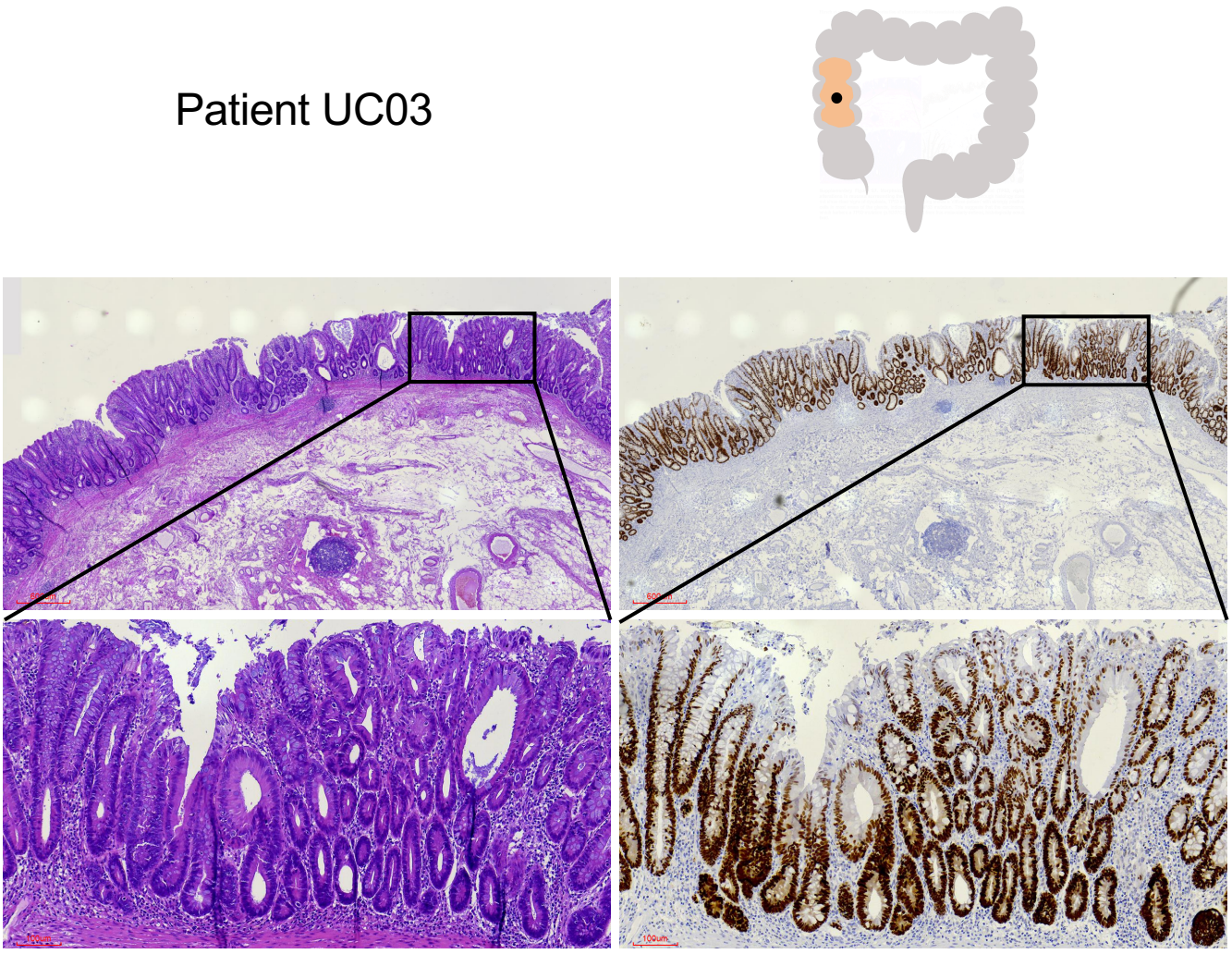

Supplementary Figure S7. Morphologic (H&E, *left*) and immunohistochemical (TP53, *right*) alterations in mucosa surrounding the carcinoma spot (indicated by black dot in the schematic, sampled surrounding mucosa area is highlighted light orange) of patient UC03. Although histology does not show clear signs of dysplasia, TP53 immunostaining shows a 'diffuse pattern' with strongly positive cells in most areas of the glands, indicative of a *TP53* mutation. This suggests that the carcinoma, which harbors a *TP53* mutation (p.R337C), emerged from this molecularly defined, histologically occult field.

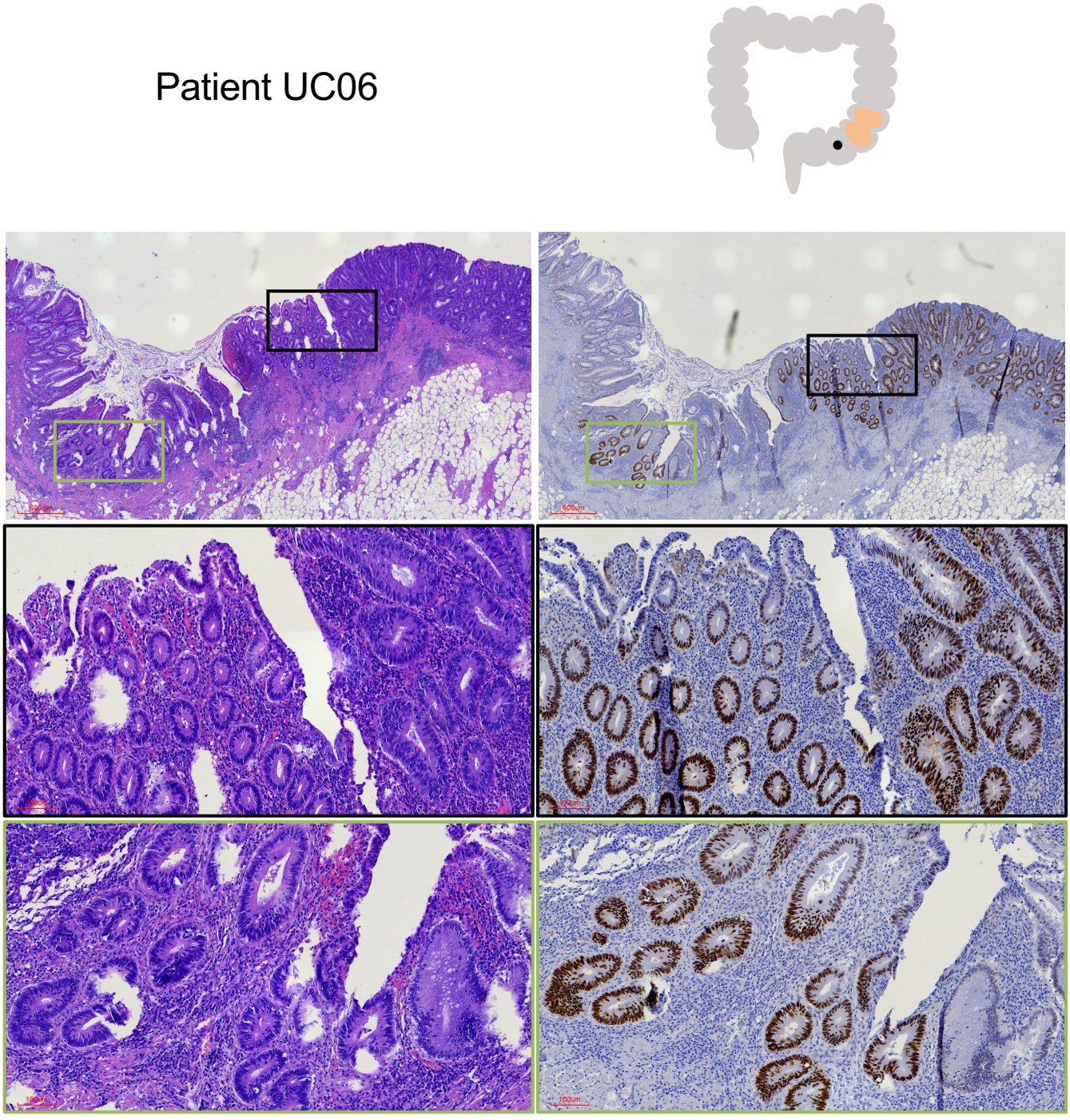

Supplementary Figure S8. Morphologic (H&E, *left*) and immunohistochemical (TP53, *right*) alterations in colonic mucosa in spatial proximity but not adjacent to the carcinoma spot (indicated by black dot in the schematic, sampled mucosa area is highlighted light orange) of patient UC06. Histology shows non-dysplastic, inflamed mucosa and low-grade dysplasia with aberrant TP53 immunostaining presenting as a 'diffuse pattern' with strongly positive cells in most areas of the glands, indicative of a *TP53* mutation. Interestingly, the carcinoma of this patient, which developed in the same bowel segment, does not show a *TP53* mutation and is instead characterized by mutations in *KRAS* and *GNAQ*.

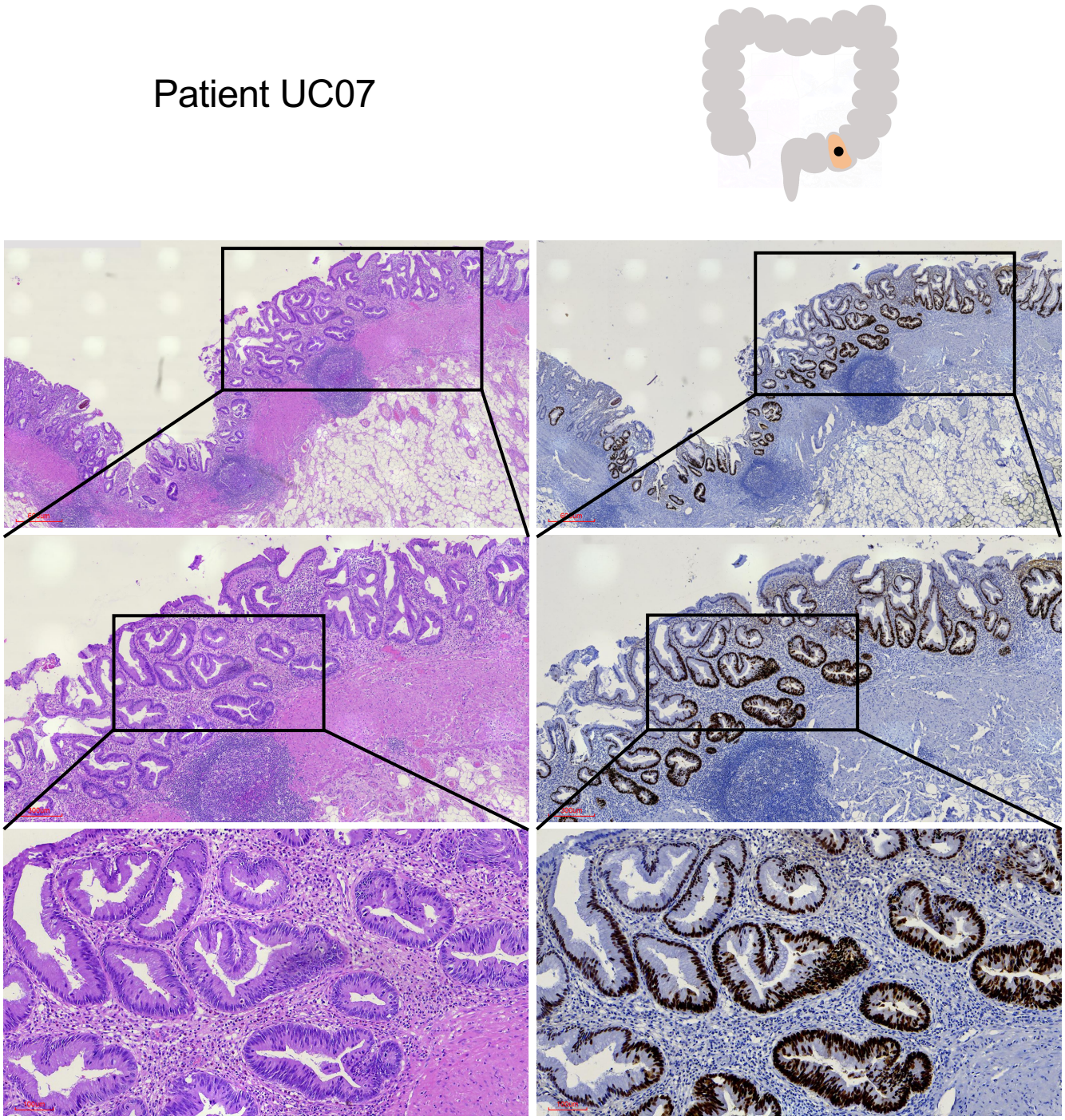

Supplementary Figure S9. Morphologic (H&E, *left*) and immunohistochemical (TP53, *right*) alterations in colonic mucosa surrounding the carcinoma spot (indicated by black dot in the schematic, sampled surrounding mucosa area is highlighted light orange) of patient UC07. Histology shows low-grade dysplasia with serrated morphology and aberrant TP53 immunostaining largely presenting as a 'nested pattern' characterized by strongly positive nuclei aggregated in restricted areas of the crypts, preferentially in the basal half of the crypts, indicative of a *TP53* mutation. The adjacent carcinoma harbors a *TP53* mutation (p.G245C), suggesting tumor progression through field cancerization.

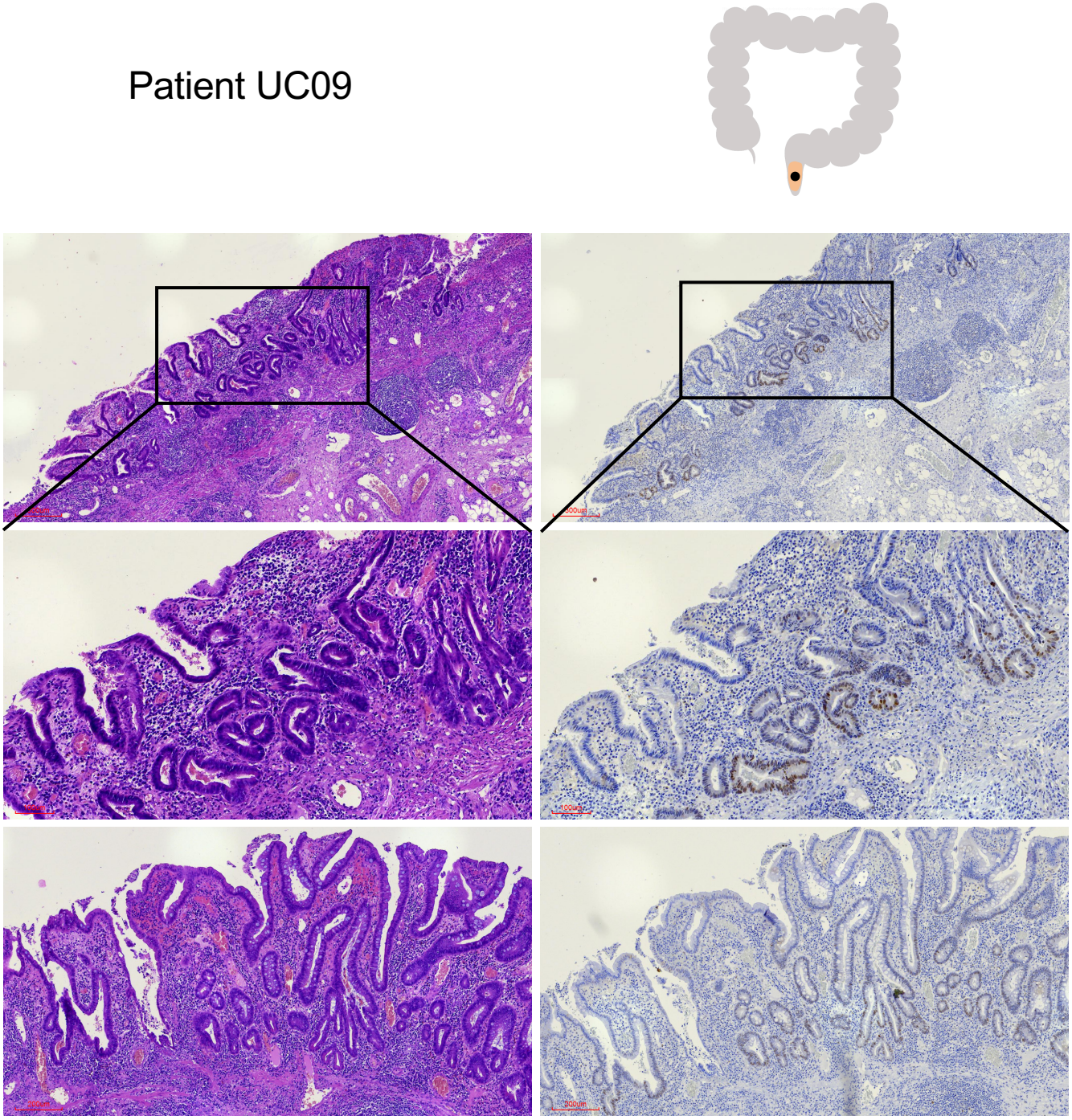

Supplementary Figure S10. Morphologic (H&E, *left*) and immunohistochemical (TP53, *right*) alterations in colonic mucosa surrounding the carcinoma spot (indicated by black dot in the schematic, sampled surrounding mucosa area is highlighted light orange) of patient UC09. Histology shows non-dysplastic, inflamed colonic mucosa. TP53 immunostaining displays a 'sporadic/scattered pattern' with only few weakly positive nuclei dispersed/focused in the crypts, indicating *TP53* wild-type status.

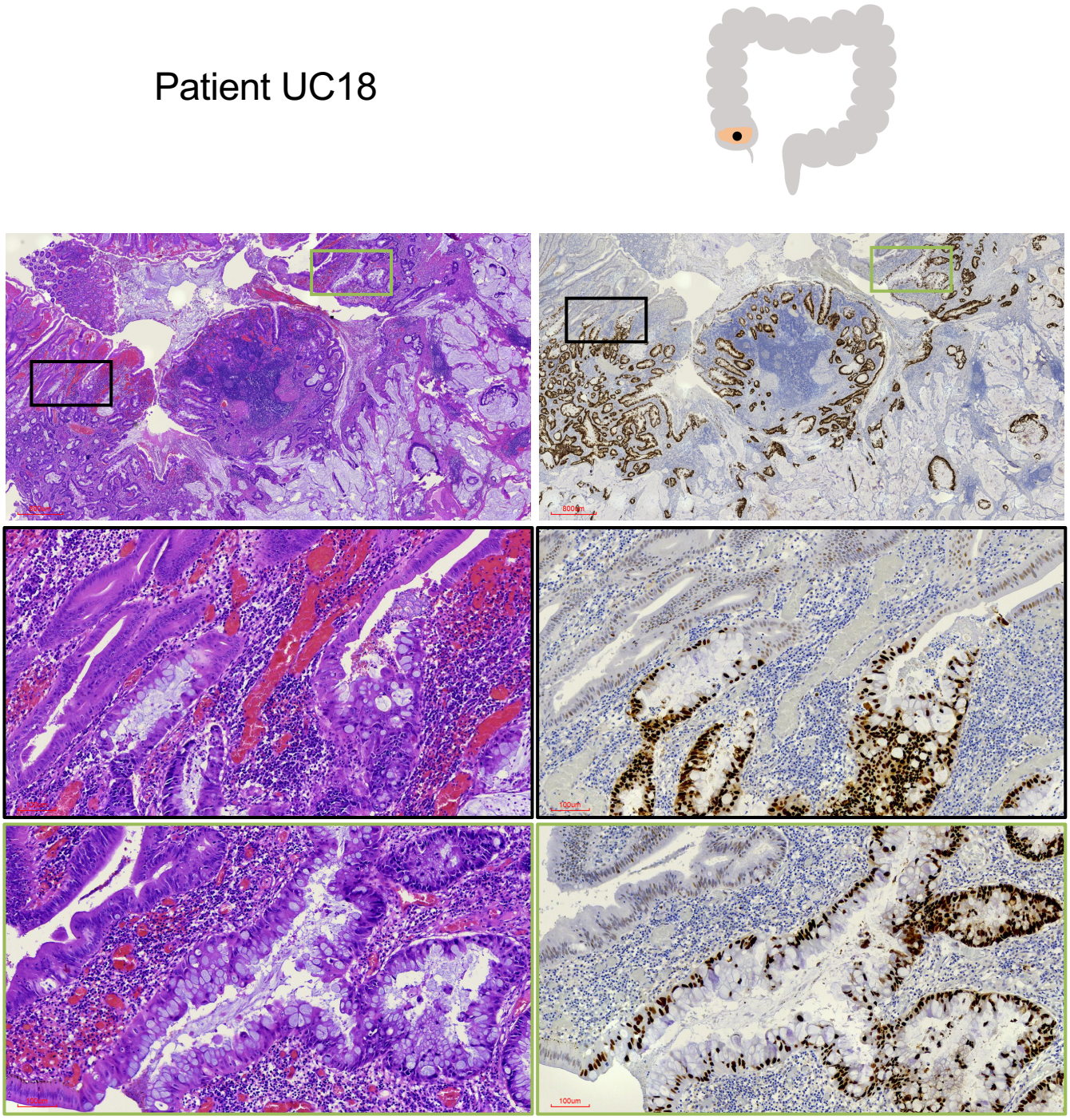

Supplementary Figure S11. Morphologic (H&E, *left*) and immunohistochemical (TP53, *right*) alterations in the carcinoma (indicated by black dot in the schematic) and adjacent colonic mucosa (highlighted in light orange in the schematic) of patient UC18. Histology and TP53 immunostaining illustrate the emergence of the carcinoma from adjacent inflamed mucosa. The neoplastic glands show an aberrant TP53 immunostaining presenting as a 'diffuse pattern' with strongly positive cells in most areas of the glands, indicative of a *TP53* mutation. This is in line with sequencing, which revealed a *TP53* mutation (p.R248Q) in the carcinoma UC18CA.